

# Impact of Rhizosphere Biostimulation on Cd Transport and Isotope Fractionation in Cd-Tolerant and Hyperaccumulating Plants Based on MC-ICP-MS and NanoSIMS

Rongfei Wei, Yizhang Liu, Fengxin Kang, Liyan Tian, Qiang Wei, Zhiying Li, Pei Xu, Huiying Hu, Qiyu Tan, Changqiu Zhao, Wei Li, and Qingjun Guo\*



Cite This: *Environ. Sci. Technol.* 2024, 58, 19408–19418



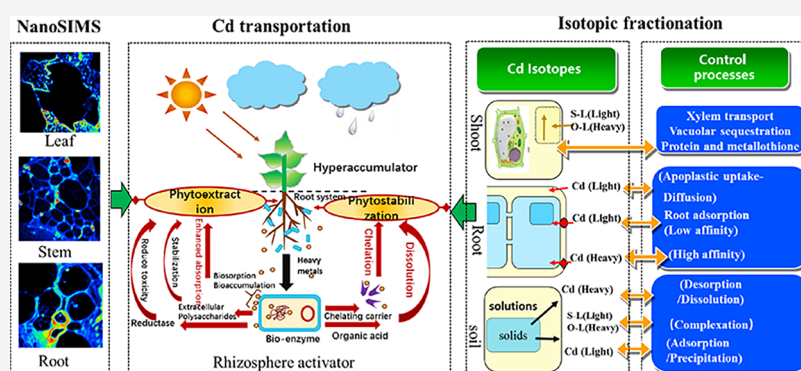
Read Online

ACCESS |

Metrics & More

Article Recommendations

Supporting Information



**ABSTRACT:** Phytoremediation efficiency can be enhanced by regulating rhizosphere processes, and the Cd isotope is a useful approach for deciphering Cd transport processes in soil–plant systems. However, the effects of adsorption and complexation on Cd isotope fractionation during the rhizosphere processes remain unclear. Here, we cultivated the Cd hyperaccumulator *Sedum alfredii* and Cd-tolerance *Sedum spectabile* in three different soils with citric acid applied as a degradable rhizosphere biostimulant. Cellular elemental distributions in the tissues and Cd isotope compositions were determined through NanoSIMS and MC-ICP-MS, respectively. Cd precipitation/adsorption on cell walls and intracellular regional distribution were the main mechanisms of Cd tolerance in *S. spectabile*. Plant roots became enriched with heavier Cd isotopes relative to the surrounding soils upon increasing secretion of rhizosphere organic acids. This indicates that organic matter with O and N functional groups preferentially chelates heavy Cd isotopes. In addition, Cd isotope fractionation between roots and shoots varies within the three soils, which could be due to the influence of protein and metallothionein contents in roots and leaves. The finding indicates that sulfur-containing ligands preferentially chelate light Cd isotopes. This study suggests that organic ligands play a vital role in Cd isotope fractionation and consequent hyperaccumulation of soil–plant systems.

**KEYWORDS:** Cd, isotope fractionation, hyperaccumulator, phytoremediation, heavy metals pollution

## 1. INTRODUCTION

Cadmium (Cd) is a toxic heavy metal with severe effects on human health, such as renal tubular dysfunction and bone disease.<sup>1,2</sup> Since the outbreak of Itai–Itai disease in Japan, Cd contamination in the food chain has emerged as a significant public health concern.<sup>3–5</sup> Consequently, remediation of Cd pollution is indispensable. Phytoremediation is a cost-effective and environmentally friendly approach for Cd-contaminated soil remediation. However, the process is hampered by inefficient in-field practices.<sup>6</sup> The extraction capacity of Cd depends on the suitability and potential of the hyperaccumulator plant or the efficiency of measurement methods. *Sedum alfredii*, a Cd hyperaccumulator, and *Sedum spectabile*, a Cd-tolerant plant, are typical hyperaccumulators due to their strong resistance and adaptability to Cd.<sup>7–9</sup>

Studying the plant rhizosphere environment could enhance remediation efficiency using phytoaccumulation.<sup>10</sup> For example, applying citrate could reactivate the antioxidant enzymes by improving their structural stability.<sup>11</sup> Do Nascimento et al.<sup>12</sup> compared the effects of natural organic acids in soils on the phytoextraction of metals from multimetal-contaminated soils and found that citric acid could efficiently remove Cd

Received: May 26, 2024

Revised: August 30, 2024

Accepted: August 30, 2024

Published: October 16, 2024



from the soil without increasing the environmental risk.<sup>11,12</sup> Lu et al.<sup>13</sup> suggested that citric acid not only participated in the absorption and transport of Cd in *S. alfredii* but also improved in the detoxification of Cd in the aboveground parts. Therefore, citric acid is a promising material for phytoremediation, rather than artificial chelating agents.

Understanding Cd enrichment and activation in hyperaccumulators or Cd-tolerant plants will have a significant role in their application in soil remediation programs. Cd hyperaccumulation and Cd tolerance of *S. alfredii* are related to absorption, transport, and detoxification mechanisms.<sup>14–17</sup> Hyperactive metal transporters and various cation detoxification pathways, such as glutathione synthesis and metal compartmentalization in vacuoles and other organelles, are responsible for the hyperaccumulation of Cd.<sup>18</sup> However, the Cd detoxification mechanisms of *S. spectabile* are not clear and need further study. The visualization of element distribution at different scales, from tissues to subcellular levels, is a crucial tool in plant science studies, since it provides insights into the detoxification mechanisms of toxic metals.<sup>19</sup> Unfortunately, Cd has relatively low secondary ion yields bombarded by O<sup>−</sup> or Cs<sup>+</sup> primary beams.<sup>19–21</sup> Therefore, there are challenges in obtaining clear Cd signals at trace levels in plant samples. With technology advancement, it becomes feasible with the nanoscale secondary ion mass spectrometry (NanoSIMS).<sup>22</sup> NanoSIMS can image charged secondary ions with a lateral resolution of less than 150 nm. This enables Cd mapping in plant tissues with high mass and high spatial resolution.<sup>19,22,23</sup>

Stable isotope techniques have been extensively used as a fingerprint to decipher the transport processes of heavy metals in soil–plant systems.<sup>24–30</sup> Heavy metal migration and transportation processes in the rhizosphere, including precipitation–dissolution, adsorption–desorption, complexation–chelation, and oxidation–reduction, could also lead to isotope fractionation of heavy metals<sup>31</sup> such as Zn,<sup>32,33</sup> Cu,<sup>34</sup> Fe,<sup>34,35</sup> and Mg.<sup>36</sup> Studies on Cd isotope fractionation in soils and plants have shown great progress with the improvement in the accuracy of Cd isotope measurement.<sup>37–41</sup> For instance, the heavy Cd isotopes in soil solutions are enriched, because they are preferentially released into aqueous phases and form stiffer bonds than those associated with the soil phase.<sup>27,30</sup> Moreover, iron minerals preferentially adsorb light Cd isotopes through equilibrium fractionation.<sup>33</sup> In addition, light Cd isotopes are also transported from solutions to accumulator plants with complexation to organic compounds.<sup>42,43</sup> Therefore, precipitation, adsorption, and complexation can also lead to Cd isotope fractionation among soils, solutions, and plants. However, the relationship between Cd isotope fractionation and Cd detoxification in hyperaccumulating plants remains unclear.

For this study, two plant species, *S. alfredii* and *S. spectabile*, were cultured in three distinct soils, and a degradable organic stimulant (citric acid) was added to the treatments during plant growth. Concentrations of Cd, Cd isotope composition, and cellular elemental distributions in the tissues were measured using multiple instruments such as inductively coupled plasma mass spectrometry (ICP-MS), multicollector inductively coupled plasma mass spectrometry (MC-ICP-MS), and nanoscale secondary ion mass spectrometry (NanoSIMS). Finally, Cd isotope fractionation is discussed in relation to soil microinterfaces, root absorption, and root-to-aboveground transport. Accordingly, this study aimed to (1) characterize Cd enrichment and its isotope fractionation from soils to

plants under rhizosphere biostimulation; (2) analyze the effects of adsorption–desorption and complexation–chelation on Cd isotope fractionation in soil–plant systems under rhizosphere biostimulation; and (3) investigate the relationship between Cd isotope fractionation and Cd availability in the soil–plant systems. Results from this study can provide technical support for improving the phytoremediation efficiency of Cd in polluted soils and enhance our understanding of the mechanisms for Cd isotope fractionation in soil–plant systems.

## 2. MATERIALS AND METHODS

**2.1. Plant Growth Experiment.** Agricultural soils were sampled from three sites in the different provinces of China: Beijing (BJ) (40°8′55.43″N, 116°14′32.80″E), Henan Province (HN) (35°8′28.58″N, 112°31′56.46″E), and Yunnan Province (YN) (26°30′55.84″N, 103°36′10.66″E). The accumulation of heavy metals at these sites possibly originates from various sources, such as agricultural practice, smelting plants, and industrial and geological contexts. The sites also varied in how soil properties affect Cd availability, due to differences in soil types (fluvo-aquic soils, cinnamon soils, and red soils), total heavy metal concentrations (e.g., Cd<sup>2+</sup>, Zn<sup>2+</sup>, and Pb<sup>2+</sup>), pH, and major ion concentrations (e.g., K<sup>+</sup>, Ca<sup>2+</sup>, Na<sup>+</sup>, Mg<sup>2+</sup>, Fe<sup>3+</sup>, and Al<sup>3+</sup>). Details on the physicochemical properties and mineral compositions of the three soils are provided in the Supporting Information (Tables S1 and S2 and Figure S1).

Prior to the experimental analysis, all collected soil samples were air-dried and sieved to <5 mm. One kilogram of dry soil from each site was placed in a plastic box and sufficiently watered with deionized water (>18.2 MΩ·cm). Three replicates were prepared for each soil sample. After 7 days, 200 mL of citric acid (100 or 400 mg/kg, coded as CA-1 and CA-2, respectively) was added to the soils. Fourteen days later, uniform plants (*S. alfredii* and *S. spectabile*) were cultivated in pots and placed in a growth chamber.

**2.2. Sample Collection and Preparation.** Plants from each experimental replicate were collected 120 days after transplantation and then thoroughly washed with tap water, followed by three rinses with deionized water. Each plant was divided into root, stem, and leaf parts. The plant materials were then freeze-dried and weighed prior to analysis. Following the method described by Wei et al.,<sup>42</sup> the plant samples were digested on a hot plate using a mixture of HNO<sub>3</sub>, HF, and HClO<sub>4</sub>. The soil samples were placed in 50 mL Teflon beakers and mixed with <sup>110</sup>Cd–<sup>111</sup>Cd double-spike solution (prepared from approximately 96.0% pure CdO) to achieve the desired Cd sample spike ratio. The samples were digested using 10–15 mL of aqua regia at 180 °C for 24 h, followed by the addition of 5 mL of concentrated HF, and then heated to dryness.

The supernatants were purified using anionic exchange chromatography with AG-MP-1 M (200–400 mesh), following the procedures described by Wei et al.<sup>42</sup> and Pallavicini et al.<sup>44</sup> The samples were purified twice to avoid isobaric element interference (e.g., by Sn) during Cd isotope analysis, as recommended by Zhang et al.<sup>45</sup> The elemental concentrations in the soils, roots, stems, and leaves were measured by using inductively coupled plasma quadrupole mass spectrometry (Elan DRC-e, PerkinElmer, USA) before and after purification. Recoveries of Cd in all samples ranged from 95 to 104%. All sample preparation was carried out in a class 100 clean room facility. The mineral acids were purified twice using sub-boiling distillation in Teflon stills. Water used in the process was of

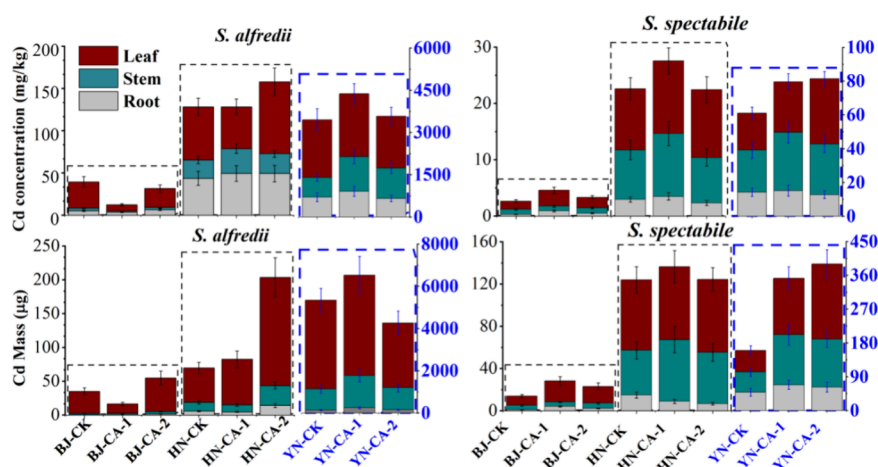


**Figure 1.** Cd concentration and Cd mass in different tissues of *S. alfredii* and *S. spectabile* activated by citric acid.

18.2 M $\Omega$ -cm purity, obtained from a Milli-Q water purification system (Millipore, Bedford, Massachusetts, USA).

**2.3. Cd Isotope Analysis.** Cd isotope ratios were measured using a Neptune Plus MC-ICP-MS (Thermo Fisher Scientific, USA) at the Institute of Geochemistry, Chinese Academy of Sciences. The procedures for Cd isotope measurements were as follows. According to the Cd concentration, standard-sample bracketing, Ag internal normalization, and double spiking were combined to correct the instrument mass bias. The true Cd isotope ratio of the double-spike solution was measured over 6 months using a Ag isotope external standard (NIST SRM 978a) to correct for instrumental mass bias.<sup>45</sup> During the analysis, NIST SRM 3108 was used as a zero internal reference standard. Three secondary Cd reference standards (Nancy Spex Cd, Spex-1 Cd, and JMC Cd) and a geological reference material (Sgr-a-1, USGS) were used to monitor the chemical separation and mass spectrometry measurements. Secondary reference standards were measured every five samples to monitor instrumental stability and reproducibility. Samples and standards were diluted to approximately 70 ng/mL using 1% HNO<sub>3</sub> (v/v) and analyzed at an uptake rate of approximately 100  $\mu$ L/min, which, generally, yielded a total Cd voltage of approximately 1.1 V for <sup>114</sup>Cd. The Cd isotope ratios for each sample were measured every 30 cycles with an internal precision of  $\pm 0.01$ – $0.02\%$  (relative standard deviation). The instrumental reproducibility based on repeated  $\delta^{114/110}\text{Cd}$  measurements of NIST SRM 3108 Cd standard solution was 0.07‰ (2SD,  $N = 214$ ). The  $\delta^{114/110}\text{Cd}_{\text{NIST 3108}}$  values of Nancy Spex Cd, Spex-1 Cd, and JMC Cd were  $-0.09 \pm 0.01$ ,  $-1.25 \pm 0.06$ , and  $4.45 \pm 0.08\%$ , respectively, which are consistent with previously reported values.<sup>42,44–46</sup> The isotope compositions are expressed in  $\delta$  (‰) relative to NIST SRM 3108. The isotope compositions are expressed in  $\delta$  (‰) relative to NIST SRM 3108:

$$\delta^{114/110}\text{Cd} = [2((^{114}\text{Cd}/^{110}\text{Cd})_{\text{sample}} / ((^{114}\text{Cd}/^{110}\text{Cd})_{\text{standard 1}} + (^{114}\text{Cd}/^{110}\text{Cd})_{\text{standard 2}}) - 1) \times 1000 \quad (1)$$

Standard 1 and standard 2 represent the standard solutions measured before and after the sample.

The  $\delta^{114/110}\text{Cd}$  values for the whole plant or shoot (stem + leaf) were calculated following Wei et al.<sup>42</sup>:

$$\delta^{114/110}\text{Cd}_{\text{whole plant or shoot}} = \frac{\sum_i m_i c_i \delta^{114/110}\text{Cd}_i}{\sum_i m_i c_i} \quad (2)$$

where  $m$ ,  $c$ , and  $i$  represent the mass of biomass (g), Cd concentration ( $\text{ng}\cdot\text{g}^{-1}$ ), and different plant parts, respectively.

The apparent isotope fractionation between the two components A and B is calculated as

$$\Delta^{114/110}\text{Cd}_{\text{A-B}} = \delta^{114/110}\text{Cd}_{\text{A}} - \delta^{114/110}\text{Cd}_{\text{B}} \quad (3)$$

**2.4. NanoSIMS Analysis of Plant Tissues.** The cellular elemental distributions in the tissues were mapped using a NanoSIMS 50L (Cameca, France) at the Institute of Surface-Earth System Science, Tianjin University. Sampling and sample preparation were performed as described previously.<sup>23,47,48</sup> Tissues approximately  $2 \times 2$  mm in size were transferred rapidly into centrifuge tubes containing 2.5% glutaraldehyde and fixed for 3 days. Subsequently, the tissues were dehydrated using a gradient of water anhydrous ethanol and gradually infiltrated with Spur resin. Afterward, the resin blocks were trimmed to a thickness of 1  $\mu\text{m}$  using an ultramicrotome and, finally, coated with a 5 nm conductive layer of Pt coating metal.

**2.5. Statistical Analysis.** Statistical analyses were performed using R free software version 4.0.3. Data were tested for normality and homoscedasticity using the Shapiro–Wilk and Bartlett tests, respectively. Variance analysis and subsequent Tukey’s honest significant difference tests were performed at a statistical significance level of  $p < 0.05$ .

### 3. RESULTS

**3.1. Enrichment Characteristics of Cd in *S. alfredii* and *S. spectabile*.** As the soil pollution level increases, the amount of Cd and its mass in the tissues of *S. alfredii* and *S. spectabile* rise in all three polluted soils (Figure 1). Regarding the two plant species, a greater Cd mass was observed in the *S. alfredii* than in *S. spectabile*, regardless of the extent of the heavy metal pollution in the soils. The findings reveal that *S. alfredii* has a stronger capacity to accumulate heavy metals than *S. spectabile*. Regarding their distribution within the tissues of the two plant species, Cd concentrations were higher in the aboveground parts of *S. spectabile* than in the roots but equal in the leaves and stems. In contrast, Cd concentrations in the tissues of *S. alfredii* decreased in the following order: leaves > stems > roots.

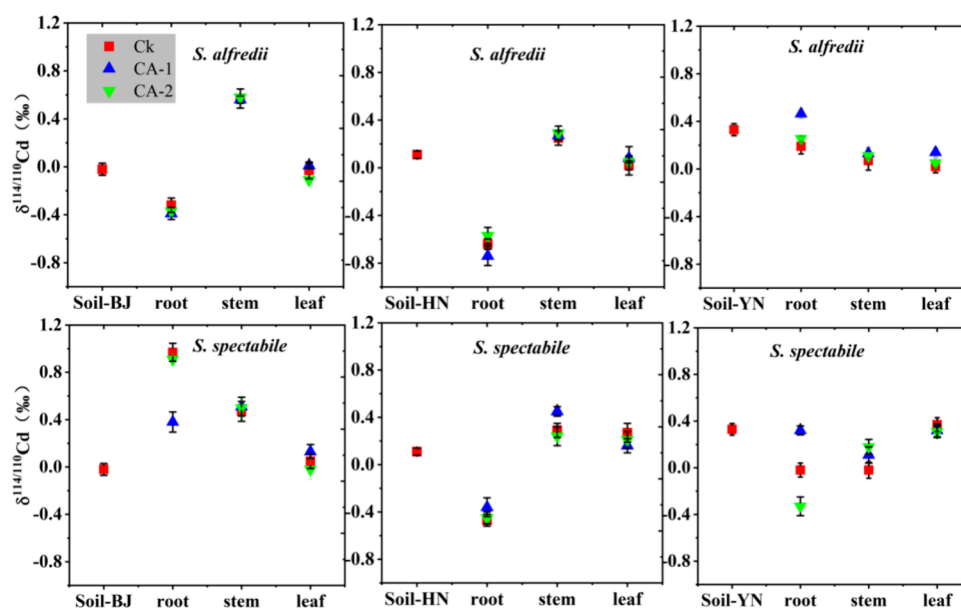


Figure 2.  $\delta^{114/110}\text{Cd}$  values of *S. alfredii* and *S. spectabile* in three agricultural soils biostimulated with citric acid treatment.

Table 1. Cd Isotope Discrimination between Different Tissues of *S. alfredii* and *S. spectabile* in the Three Types of Soils during the Citric Acid Treatments

$\Delta^{114/110}\text{Cd}$	treatments	root–soil	stem–soil	leaf–soil	plant–soil	shoot–soil	root–plant	shoot–plant	shoot–root	leaf–stem
<i>S. alfredii</i>	BJ-CK	−0.30	0.59	−0.01	0.02	0.03	−0.32	0.01	0.33	−0.60
	BJ-CA-1	−0.37	0.58	0.03	0.06	0.09	−0.43	0.03	0.46	−0.55
	BJ-CA-2	−0.35	0.60	−0.09	−0.05	−0.04	−0.30	0.01	0.31	−0.69
	HN-CK	−0.75	0.14	−0.09	−0.10	−0.04	−0.65	0.06	0.71	−0.23
	HN-CA-1	−0.85	0.16	−0.03	−0.05	0.00	−0.80	0.05	0.85	−0.19
	HN-CA-2	−0.68	0.18	−0.06	−0.07	−0.02	−0.61	0.05	0.66	−0.24
	YN-CK	−0.14	−0.26	−0.31	−0.30	−0.30	0.16	0.00	−0.16	−0.05
	YN-CA-1	0.13	−0.20	−0.19	−0.18	−0.19	0.31	−0.01	−0.33	0.01
	YN-CA-2	−0.08	−0.22	−0.28	−0.26	−0.26	0.18	−0.01	−0.19	−0.06
<i>S. spectabile</i>	BJ-CK	0.99	0.49	0.07	0.27	0.20	0.72	−0.06	−0.79	−0.42
	BJ-CA-1	0.40	0.53	0.15	0.24	0.22	0.16	−0.03	−0.18	−0.38
	BJ-CA-2	0.93	0.52	0.00	0.22	0.13	0.71	−0.09	−0.80	−0.52
	HN-CK	−0.58	0.18	0.16	0.08	0.17	−0.66	0.09	0.75	−0.02
	HN-CA-1	−0.69	0.12	−0.17	−0.08	−0.04	−0.61	0.04	0.65	−0.29
	HN-CA-2	−0.78	−0.09	−0.12	−0.14	−0.11	−0.64	0.04	0.67	−0.03
	YN-CK	−0.35	−0.35	0.04	−0.21	−0.15	−0.14	0.06	0.20	0.39
	YN-CA-1	−0.01	−0.22	−0.01	−0.09	−0.11	0.08	−0.02	−0.10	0.21
	YN-CA-2	−0.66	−0.15	−0.02	−0.16	−0.07	−0.50	0.09	0.59	0.13

Regarding the role of biostimulant concentration, the Cd accumulation potential of *S. alfredii* and *S. spectabile* was enhanced with the addition of citric acid. In BJ and HN soils, *S. spectabile* exhibited the highest Cd accumulation at low concentrations of citric acid, whereas *S. alfredii* showed fairly good accumulation at high concentrations. In contrast, in YN soils, accumulated Cd in *S. spectabile* was high under a high citric acid concentration, whereas there was an excellent accumulation in *S. alfredii* at a low citric acid concentration.

**3.2. Cd Isotope Composition in *S. alfredii* and *S. spectabile* Activated by Citric Acid.** Variations in Cd isotopes were most pronounced in the roots of the two plant species after stimulation by citric acid (Figure 2). Moreover, the isotope compositions varied within the soil types. In BJ soils, the roots of both plant species were enriched with light Cd isotopes, while in YN and HN soils, the roots of *S. alfredii* and *S. spectabile* were enriched with heavy Cd isotopes. The Cd

isotope values in the roots of *S. alfredii* in HN soils and *S. spectabile* in YN soils varied depending on the amount of citric acid added. Thus, the addition of citric acid in BJ and YN soils led to the largest change in the Cd isotope value in the roots of *S. spectabile* in BJ and YN soils. Overall, the variation in Cd isotope values in these plant species depends on factors such as tissue types, concentrations of citric acid, soil properties, and element concentrations.

**3.3. Cd Isotope Fractionation between Different Tissues of *S. alfredii* and *S. spectabile*.** As shown in Table 1, the  $\Delta^{114/110}\text{Cd}$  value differed substantially between *S. alfredii* and *S. spectabile* in the three distinct soils. *S. alfredii* exhibited an enrichment of light Cd isotopes from the soils to the roots ( $\Delta^{114/110}\text{Cd}_{\text{root-soil}} = -0.85$  to  $-0.08\text{‰}$ ), except for YN soils with a low citric acid concentration ( $0.13\text{‰}$ ). In contrast, a depletion of light Cd isotopes was observed from roots to shoots ( $\Delta^{114/110}\text{Cd}_{\text{shoot-root}} = 0.01$  to  $0.85\text{‰}$ ) in BJ and



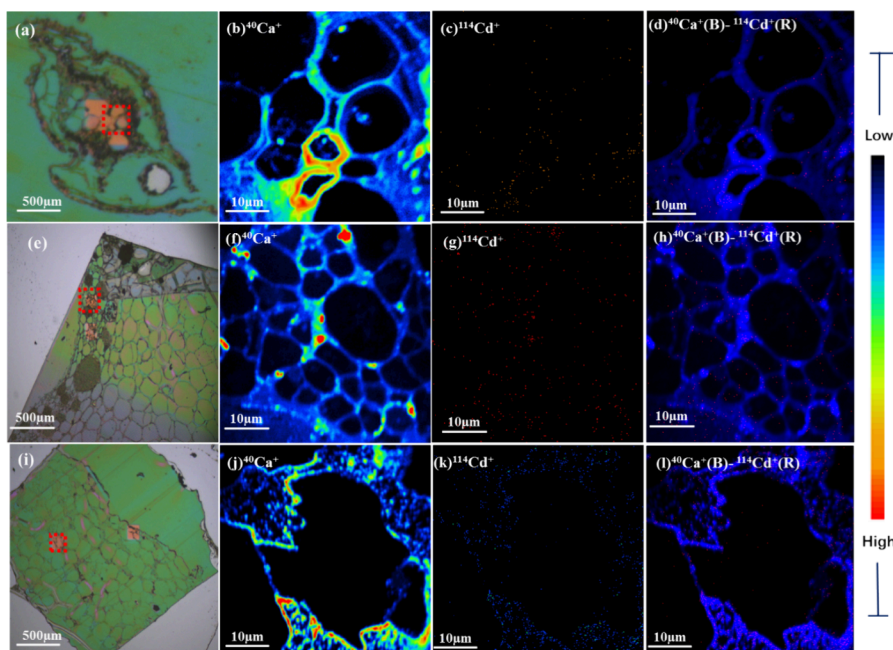


**Figure 3.** NanoSIMS elemental maps ( $10\ \mu\text{m} \times 10\ \mu\text{m}$ ) of *S. spectabile* tissues, with (a–d) showing the elemental maps of roots, (e–h) showing the elemental maps of stems, (i–l) showing the elemental maps of leaves, and (d, h, and l) showing the composite (multi)elemental maps of *S. spectabile*, indicating the relative location of Cd (red) and Ca (blue).

HN soils, while an enrichment was seen from roots to shoots in YN soils ( $\Delta^{114}\text{Cd}_{\text{shoot-root}} = -0.33$  to  $-0.16\%$ ). In *S. alfredii*, positive or negative shifts in the isotope ratios from roots to shoots and soils to roots were more pronounced in HN soils ( $\Delta^{114/110}\text{Cd}_{\text{root-soil}} = -0.85$  to  $-0.68\%$ ;  $\Delta^{114/110}\text{Cd}_{\text{shoot-root}} = 0.66$  to  $0.85\%$ ) compared to YN soils.

*S. spectabile* exhibited an enrichment of light Cd isotope composition from soils to roots in both HN and YN soils ( $\Delta^{114/110}\text{Cd}_{\text{root-soil}} = -0.78$  to  $-0.01\%$ ) but an enrichment of heavy Cd isotope composition in BJ soils ( $\Delta^{114/110}\text{Cd}_{\text{root-soil}} = 0.40$  to  $0.99\%$ ). On the other hand, *S. spectabile* exhibited an enrichment in light Cd isotope composition from roots to shoots in BJ soils ( $\Delta^{114/110}\text{Cd}_{\text{shoot-root}} = -0.80$  to  $-0.18\%$ ) and an enrichment of heavy Cd isotope composition in HN and YN soils ( $\Delta^{114/110}\text{Cd}_{\text{shoot-root}} = 0.20$  to  $0.75\%$ ), except for YN soils under a low citric acid concentration ( $\Delta^{114/110}\text{Cd}_{\text{shoot-root}} = -0.10\%$ ). In *S. spectabile*, positive or negative shifts of the isotope ratios were less pronounced from roots to shoots ( $\Delta^{114/110}\text{Cd}_{\text{root-soil}} = -0.66$  to  $-0.10\%$ ) and soils to roots ( $\Delta^{114/110}\text{Cd}_{\text{shoot-root}} = -0.10$  to  $0.59\%$ ) in YN soils.

The values of  $\Delta^{114/110}\text{Cd}_{\text{leaf-stem}}$  in the two plant species showed an order of BJ < HN < YN. *S. alfredii* exhibited an enrichment of light Cd isotopes from stems to leaves ( $\Delta^{114/110}\text{Cd}_{\text{leaf-stem}} = -0.69$  to  $0.01\%$ ). Negative shifts in the isotope ratios between stems and leaves were more pronounced in BJ soils for *S. alfredii*. In contrast to *S. alfredii*, *S. spectabile* exhibited an enrichment in light Cd isotopes from stems to leaves in BJ and HN soils ( $\Delta^{114/110}\text{Cd}_{\text{leaf-stem}} = -0.48$  to  $-0.02\%$ ) but an enrichment of heavy Cd isotopes was found in the YN soils ( $\Delta^{114/110}\text{Cd}_{\text{leaf-stem}} = 0.13$  to  $0.39\%$ ).

## 4. DISCUSSION

**4.1. Subcellular Localization and Detoxification Mechanism of *S. alfredii* and *S. spectabile*.** In *S. spectabile*, 44.06–53.47% of the Cd in the leaves is distributed in cellular debris, which includes the cell wall and cell membrane.<sup>49,50</sup>

Moreover, *S. spectabile* exhibited a greater Cd accumulation with a large proportion of it in the cellular debris.<sup>50</sup> Therefore, the cell wall could be an important barrier separating protoplasts to alleviate Cd toxicity in plants. In this study, the cellular elemental distributions in the roots, stems, and leaves of *S. spectabile* were determined using a NanoSIMS (Figure 3). The images of a, e, and i in Figure 3 show the structure and integrity of the plant tissue surface. An O-ion beam was scanned across the surface of a section and positive ion elemental maps were obtained. Similar to the  $^{12}\text{C}^{14}\text{N}^-$  image, the  $^{40}\text{Ca}^+$  image was typically used to illustrate morphology in organic materials, and here it reveals the cell wall outline and some intracellular structure.<sup>21,51</sup> The  $^{114}\text{Cd}^+$  and composite ( $^{114}\text{Cd}^+$  and  $^{40}\text{Ca}^+$ ) images displayed a strong enrichment of Cd in the cell walls of the plant tissues (Figure 3). Cd in the root, stem, and leaf cells of *S. spectabile* was primarily distributed in the cell wall and intercellular space, with relatively little Cd content in the cytoplasm. Such phenomenon was more obvious in the leaf cell wall, which could be attributed to higher Cd concentration in the leaf than in the root cells. This study confirmed that Cd precipitation and adsorption processes in the cell wall, as well as Cd distribution in the intracellular region, were the main mechanisms contributing to the Cd tolerance of *S. spectabile*. Unlike *S. spectabile*, Cd in *S. alfredii* was predominantly found in the mesophyll and vascular cells of the leaves rather than the epidermis, and it preferentially accumulated in the pith and cortex of the stems.<sup>52</sup>

To date, Cd localization in tissues has been investigated in several plant species, including Cd hyperaccumulators, Cd-tolerant plants, crops, and vegetables (such as *Thlaspi caerulescens*, *Arabidopsis thaliana*, chili, and foliar).<sup>47,52,53</sup> Cd absorption, transport, and detoxification mechanisms include the following processes<sup>14–17</sup>: (1) precipitation and adsorption at root cell walls; (2) intracellular regionalized distribution (vacuolar sequestration) by tonoplast-located transporters; (3)

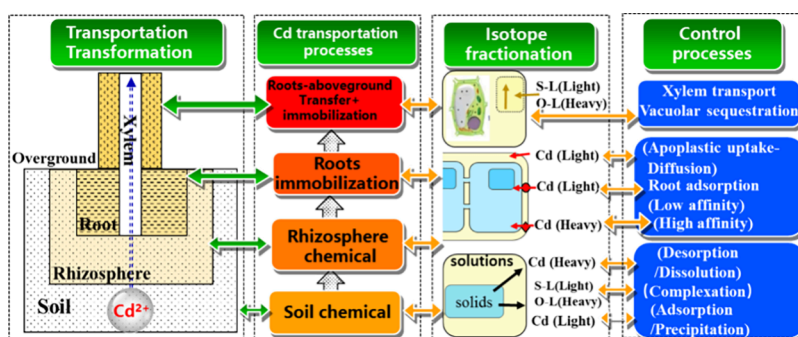


**Figure 4.** Cd transportation and isotope fractionation in soil–plant systems (S-L: sulfur-containing ligands; O-L: oxygenated ligands)<sup>26–30,59–64,70–72</sup>

chelation of metals in the cytosol by peptides such as phytochelatins; and (4) effects of the enzyme system. With regard to Cd hyperaccumulators, Cd detoxification in the roots of *Thlaspi caerulescens* is localized in both the apoplast (e.g., binding to cell-wall compounds) and inside cells, whereas vacuoles serve as the primary compartments for Cd storage and cation detoxification in leaves.<sup>54,55</sup> *Arabidopsis thaliana* retains Cd in its roots and leaves primarily through vacuolar sequestration and cytoplasmic precipitation.<sup>52,53</sup> Moreover, Cd is typically localized in the cell wall fraction of lettuce, Cd-resistant barley genotypes, water spinach (*Ipomoea aquatica* Forsk, WS), and pak choi (*Brassica chinensis* L., PC),<sup>23,56,57</sup> and associated with pectates and proteins in the soluble and cell wall fractions.

Lu et al.<sup>58</sup> noted that Cd primarily enters into the stele of *S. alfredii* roots through a symplastic pathway, and is subsequently translocated to the shoots. Cd in the leaves of *S. alfredii* is mainly stored in the vacuoles, which contain a large amount of malic acid. Therefore, detoxification in *S. alfredii* occurs via binding of Cd with malic acid but not with most sulfur-containing sulfhydryl compounds. Nevertheless, some sulfhydryl compounds do participate in the Cd detoxification mechanisms in the roots.<sup>52</sup> However, the current study found that more Cd accumulated in the cell debris of *S. spectabile* and biologically detoxified metal fractions compared to that in *S. alfredii*. This finding suggests that the Cd binding to the cell wall, phytochelatins, and metallothioneins (MT) in *S. spectabile* could indicate internal detoxification mechanisms. Accordingly, Cd mainly binds to oxygen-containing ligands in the xylem of *S. alfredii*, whereas it binds to sulfur-containing ligands in *S. spectabile*.

**4.2. Cd Isotope Fractionation in Soil Rhizosphere Processes under Organic Acid Stimulation.** The  $\delta^{114/110}\text{Cd}$  values in BJ, HN, and YN soils were  $-0.02 \pm 0.05$ ,  $0.11 \pm 0.03$ , and  $0.33 \pm 0.05\text{‰}$ , respectively, and the average  $\Delta^{114/110}\text{Cd}_{\text{WP-soil}}$  values were 0.01,  $-0.07$ ,  $-0.24\text{‰}$  and 0.24,  $-0.05$ , and  $-0.16\text{‰}$  for *S. alfredii* and *S. spectabile*, respectively (Table 1). The average  $\Delta^{114/110}\text{Cd}_{\text{WP-soil}}$  values for the two plant species in the three distinct soils decreased in the order of BJ > HN > YN. An enrichment of light Cd isotopes was found in HN and YN soils while an enrichment of heavy Cd isotopes was found in BJ soils in both plant species. There is a strong correlation between fractionation and soil types. In addition, the magnitudes of isotopic shifts during solution-to-organ transfer increased slightly when Cd concentrations in the tissues decreased.<sup>42</sup> In this study, the relatively less distinct isotope fractionation between the soils and roots (as well as roots and shoots) in the two selected plant species in YN soils

validates the aforementioned conclusion. This implies that the alteration in the isotope ratio is minor when plants experience poor growth in highly polluted environments.

As shown in Figure S2, the  $\Delta^{114/110}\text{Cd}_{\text{root-soil}}$  values did not show a significant correlation with the BCF of roots in the two plant species. This finding indicates that Cd isotope fractionation is influenced not only by root uptake but also by soil physicochemical properties and rhizosphere exudates and possibly other factors. The availability of Cd in soil solution is influenced mainly by factors such as levels of iron and manganese oxide, cadmium sulfide, and organic matter. As shown in Figure S3, Cd in HN and YN soils is primarily iron–manganese oxide-bound Cd (34.5–57.7%) and exchangeable Cd (30.9–53.8%). In contrast to the above two soils, most of the Cd in BJ soils exists bound to iron–manganese oxide (42.9–87.4%) and carbonate (3.4–36.6%), but no Cd exists in an exchangeable phase. After harvesting the two plant species, the concentration of the exchangeable Cd decreased, while the concentration of the organically bound Cd increased in both HN and YN soils. In contrast to the two soils, the concentration of the carbonate-bound Cd and iron–manganese oxide-bound Cd decreased, whereas the concentration of organically bound Cd exhibited a slight fluctuation. Therefore, the two plant species mainly utilized exchangeable Cd in HN and YN soils, while they initially utilized carbonate-bound Cd and iron–manganese oxide-bound Cd in BJ soils. Based on this, the adsorption and precipitation of iron–manganese binders primarily affected Cd in BJ soils, while the dissolution of exchangeable Cd and the complexation of organically bound substances also had a significant impact in HN and YN soils.

The movement and availability of heavy metals in soils are related to their speciation, which is influenced by processes of precipitation and dissolution, adsorption and desorption, and complexation (Figure 4).<sup>59–64</sup> These processes can be influenced by the physicochemical properties of soils, such as pH, mineral composition, organic matter, and redox conditions.<sup>59,60</sup> Previous studies have shown that heavy Cd isotopes are released into soil solutions from the soil solid phase during desorption and dissolution, whereas light Cd isotopes are produced during precipitation and adsorption processes.<sup>61–64</sup> Horner et al.<sup>65</sup> and Yang et al.<sup>66</sup> suggested that sulfur-containing organic matter tends to bind light Cd isotopes, while organic matter with an oxygen-containing functional group tends to complex heavy Cd isotopes.<sup>67</sup> All of these processes support the results of the present study, specifically the reason that  $\Delta^{114/110}\text{Cd}_{\text{WP-soil}}$  values in BJ soils

for *S. alfredii* and *S. spectabile* were greater than those in YN soils.

Furthermore, in our study, low citric acid concentrations activated Cd in rhizosphere soils and enhanced the absorption efficiency of *S. alfredii* and *S. spectabile* in YN soils (unpublished data). The roots of both species became enriched with heavy Cd isotopes in YN soils, indicating that root absorption caused the enrichment of heavy Cd isotopes. In addition, the roots of *S. alfredii* in YN soils under low citric acid concentrations (Figure S4) and the roots of *S. spectabile* in BJ soils secreted more low-molecular-weight organic acids. It indicates that the complexation of organic acid led to the enrichment of heavy Cd isotopes in the roots. This finding confirms that organic matter containing functional groups of oxyl groups preferentially chelates heavy Cd isotopes. The effects of citric acid on the Cd isotope composition were more pronounced in the roots than in the stems and leaves of both plant species. The major plant-induced processes responsible for metal mobilization include rhizosphere acidification and the exudation of organic ligands with the first process causing the dissolution of metal-bearing phases and the second leading to the complexation of metals in soil solution.<sup>68</sup> Consistent with the current study, our earlier research showed that ethylenediaminetetraacetic acid (EDTA) could bind heavy Cd isotopes and allow light Cd isotopes to be preferentially taken up by *R. communis* and *S. nigrum*.<sup>42</sup>

#### 4.3. Cd Isotope Fractionation during Root Uptake.

Plant roots absorb Cd through the following two main processes. The first is abiotic, which involves Cd diffusion, adsorption, and precipitation on the soil and root surface. The second is biological, encompassing ion channels, electrochemical potential differences inside and outside the cytoplasm, and transporters. Diffusion can lead to light Cd isotope fractionation (Figure 4).<sup>31</sup> Our previous study revealed the effects of ion diffusion on Cd isotope fractionation in *R. communis* and *S. nigrum* during both low- and high-Cd treatments.<sup>67</sup> In the second process, ion channels and electrochemical potential differences inside and outside the cytoplasm lead to Cd isotope fractionation. In contrast, an enrichment of light Cd isotopes occurred during low-affinity transport (e.g., ion channels and electrogenic pumps), while the opposite was observed for high-affinity transport (e.g., ion carriers) (Figure 4).<sup>24–30</sup> When heavy metals in soil solutions diffuse into plant roots, they first react with the root system's cell walls.

In this study, an enrichment of light Cd isotopes was found from soils to roots in all *S. alfredii* treatments, except YN, with a low citric acid concentration and in *S. spectabile* for both HN and YN soils. However, an enrichment of heavy Cd isotopes from soils to roots, along with high rhizosphere secretion of organic acids, was found in the remaining treatments (Figure S4). These findings suggest that heavier Cd isotopes are enriched in soils, where more rhizosphere organic acids are secreted by the root systems. Rhizosphere organic acids can lower the pH of the surrounding environment. In addition, organic ligands can bind to heavy metals in soil solutions. These processes could promote the release of heavy metals from the soil's solid phase.<sup>69</sup> Organic acids preferentially bind to light Cd isotopes, and heavy Cd isotopes are absorbed by plant roots, resulting in an enrichment of heavy isotopes in the roots with more rhizosphere organic acid secretion. These findings corroborate our conclusion that the oxygen-containing

ligands, such as citric and malic acids, tend to bind heavy Cd isotopes from soils to roots.

**4.4. Cd Isotope Fractionation from Root to Above-ground Transport.** As shown in Figure S5, the  $\Delta^{114/110}\text{Cd}_{\text{stem-root}}$  and  $\Delta^{114/110}\text{Cd}_{\text{leaf-stem}}$  values in *S. alfredii* exhibited significant correlations with the  $\text{TF}_{\text{root-stem}}$  and  $\text{TF}_{\text{stem-leaf}}$  but no correlations were observed in the tissues of *S. spectabile*. This finding suggests that Cd transfer processes within the various parts of *S. alfredii* may significantly influence its isotope fractionation, as *S. alfredii* accumulated more Cd compared to *S. spectabile*. The  $\Delta^{114/110}\text{Cd}_{\text{root-soil}}$  and  $\Delta^{114/110}\text{Cd}_{\text{leaf-soil}}$  values did not correlate with the BCF values of the roots and leaves in both plant species, whereas the  $\Delta^{114/110}\text{Cd}_{\text{stem-soil}}$  value was significantly correlated with the BCF values of the stem (Figure S2). This result indicates that the Cd isotope fractionation from soils to roots or to leaves is not solely affected by Cd transfer processes.

In Figure S6, the  $\Delta^{114/110}\text{Cd}_{\text{plant/shoot-root}}$  values in *S. alfredii* were strongly correlated with the Cd mass of plant tissues, whereas there was no correlation between the  $\Delta^{114/110}\text{Cd}_{\text{leaf-stem}}$  values and the Cd mass of tissues. In contrast, the Cd isotope fractionation between soils and *S. spectabile* showed no strong correlations with the weight and Cd mass of plant tissues while the  $\Delta^{114/110}\text{Cd}_{\text{leaf-stem}}$  values for *S. spectabile* showed strong correlations with the height of plants.

Metal isotope fractionation between roots and shoots is primarily governed by root sequestration (such as adsorption to the apoplast and chelation with organic ligands in vacuoles) and the root-to-shoot translocation processes (xylem loading).<sup>73</sup> Vacuolar sequestration refers to Cd transport from the root cytoplasm to the vacuoles. During this process, Cd can be complexed with plant-chelated peptides and sulfur-based ligands, such as metallothionein,<sup>65</sup> which tends to the enrichment of light Cd isotopes.<sup>70,74</sup> During xylem loading, Cd migrates from the transpiration stream to the leaf via the xylem.<sup>75</sup> Our previous study revealed that Cd isotope fractionation differed between the roots and leaves of *R. communis* and *S. nigrum*. This variation was attributed to the higher proportion of oxygen-containing ligands chelated by the cell walls in hyperaccumulator plants (*S. nigrum*), whereas sulfur-containing ligands chelated by vacuoles were predominant in tolerant plants (*R. communis*).<sup>42,76,77</sup> Moreover, oxygen-containing ligands tend to be enriched with heavy isotopes, while sulfur-containing ligands are enriched with light isotopes.<sup>61</sup> Therefore, the Cd isotope composition in *S. nigrum*'s leaves becomes heavier relative to stems, whereas lighter from stems to leaves for *R. communis*.

In this study, Cd exported to shoots was isotopically heavier than the Cd pools in the roots of *S. alfredii* (BJ and HN soils) ( $\Delta^{114/110}\text{Cd}_{\text{shoot-root}} = 0.01$  to  $0.85\%$ ) and *S. spectabile* (HN and YN soils) ( $\Delta^{114/110}\text{Cd}_{\text{shoot-root}} = 0.20$  to  $0.75\%$ ). This result is consistent with previous results for rice ( $\Delta^{114/110}\text{Cd}_{\text{shoot-root}} = 0.22$  to  $0.32\%$ ),<sup>30</sup> wheat,<sup>70,74</sup> *R. communis*, and *S. nigrum*.<sup>42</sup> In contrast, the shoots of *S. alfredii* (YN soil) ( $\Delta^{114}\text{Cd}_{\text{shoot-root}} = -0.33$  to  $-0.16\%$ ) and *S. spectabile* (BJ soils) ( $\Delta^{114/110}\text{Cd}_{\text{shoot-root}} = -0.80$  to  $-0.18\%$ ) exhibited enrichment of lighter Cd isotopes than to their respective roots. In addition, the  $\Delta^{114/110}\text{Cd}_{\text{leaf-stem}}$  values in *S. alfredii* were lighter than those of *S. spectabile*. Moreover, the leaves of the two plant species in all treatments were enriched in light Cd isotopes relative to the stems, except the leaves of *S. spectabile*, which showed heavy Cd isotope enrichment relative



to the stems. Notably, the metallothionein (MT) concentrations in the leaves of *S. spectabile* were significantly lower than those in the leaves of *S. alfredii* (Figure S7). This suggests that Cd in the leaves of *S. alfredii* leaves might preferentially bind to MTs. MTs in plants usually possess a high proportion of cysteine, a thiol-containing amino acid, and can form metal–thiolate clusters to eliminate toxicity of heavy metals.<sup>78–80</sup> Similarly, the protein concentrations of *S. spectabile* in YN soils were the lowest. The  $\Delta^{114/110}\text{Cd}_{\text{leaf-stem}}$  values of the two plant species were affected by the protein and MT contents of the leaves, with the results showing that the protein and MT preferentially chelate with light Cd isotopes. Consistent with this, Zhong et al.<sup>80</sup> suggested that Cd immobilization through binding to MTs may favor the enrichment of lighter Cd isotopes in older leaves of rice. Therefore, the results confirm that sulfur-containing ligands preferentially chelate light Cd isotopes.

**4.5. Environmental Implications.** Phytoremediation technology is an effective technique in CO<sub>2</sub> fixation. Plants directly absorb pollutants or enhance their removal indirectly, contributing to environmental remediation and carbon neutrality. Based on the phytoremediation of the two typical plant species, this study investigated how rhizosphere biostimulation influences the relationships between Cd isotope fractionation and Cd availability in soil–plant systems. First, the precipitation or adsorption of Cd on cell walls and its intracellular regional distribution were the main mechanisms of Cd tolerance in *S. spectabile*. This finding showed the effectiveness of the plants in remediating heavy-metal-contaminated soils and enhanced their phytoremediation efficiency. For example, increasing the contents of polysaccharides, proteins, lignin, and other components can promote the aggregation of heavy metals in the cell walls, thereby preventing their entry into the cytoplasm and causing damage to plants. Additionally, the root system became enriched with heavy Cd isotopes relative to the soil when more rhizosphere organic acids were secreted. This finding confirms that organic matter containing O and N functional groups preferentially chelates heavy Cd isotopes. Moreover, Cd isotope fractionation between the roots and shoots of *S. alfredii* and *S. spectabile* differed among the soil types. This phenomenon could be related to the protein and MT contents of the roots/leaves, confirming that sulfur-containing ligands preferentially chelate light Cd isotopes. Therefore, this research suggests that organic ligands play a vital role in Cd isotope fractionation of soil–plant systems. Overall, this study enhances our understanding of the mechanisms involved in Cd isotope fractionation during Cd enrichment, migration, and translocation in soil–plant systems that are activated by biostimulation.

## ■ ASSOCIATED CONTENT

### SI Supporting Information

The Supporting Information is available free of charge at <https://pubs.acs.org/doi/10.1021/acs.est.4c03674>.

Description of additional experimental methods; soil properties, element concentrations, and mineralogical compositions of soils; the transfer factors (TF) and enrichment coefficient factors (BCF); correlation analyses among the weight, Cd mass, TF, BCF, and  $\Delta^{114/110}\text{Cd}$  from the different tissues of plants; Cd proportion in different chemical fractions of soils;

exudation of LMWOAs secreted by roots; the protein concentration and MT content of leaves (PDF)

## ■ AUTHOR INFORMATION

### Corresponding Author

**Qingjun Guo** – Institute of Geographic Sciences and Natural Resources Research, Chinese Academy of Sciences, Beijing 100101, China; College of Resources and Environment, University of Chinese Academy of Sciences, Beijing 100101, China; [orcid.org/0000-0003-1538-1339](https://orcid.org/0000-0003-1538-1339); Phone: +86-10-64889455; Email: [guojq@igsnrr.ac.cn](mailto:guojq@igsnrr.ac.cn); Fax: +86-01-64889455

### Authors

**Rongfei Wei** – Institute of Geographic Sciences and Natural Resources Research, Chinese Academy of Sciences, Beijing 100101, China; [orcid.org/0009-0002-8050-3961](https://orcid.org/0009-0002-8050-3961)

**Yizhang Liu** – Institute of Geochemistry, Chinese Academy of Sciences, Guiyang 550002, China

**Fengxin Kang** – Institute of Geographic Sciences and Natural Resources Research, Chinese Academy of Sciences, Beijing 100101, China

**Liyan Tian** – Institute of Process Engineering, Chinese Academy of Sciences, Beijing 100101, China

**Qiang Wei** – Institute of Geographic Sciences and Natural Resources Research, Chinese Academy of Sciences, Beijing 100101, China

**Zhiying Li** – School of Geography and Information Engineering, China University of Geosciences, Wuhan 430074, China

**Pei Xu** – Institute of Geographic Sciences and Natural Resources Research, Chinese Academy of Sciences, Beijing 100101, China

**Huiying Hu** – Institute of Geographic Sciences and Natural Resources Research, Chinese Academy of Sciences, Beijing 100101, China

**Qiyu Tan** – School of Ecology and Environmental Sciences, Yunnan University, Kunming 650091, China

**Changqiu Zhao** – Institute of Geographic Sciences and Natural Resources Research, Chinese Academy of Sciences, Beijing 100101, China; [orcid.org/0000-0001-6180-0667](https://orcid.org/0000-0001-6180-0667)

**Wei Li** – School of Earth Sciences and Engineering, Nanjing University, Nanjing 230046, China; [orcid.org/0000-0002-0789-0320](https://orcid.org/0000-0002-0789-0320)

Complete contact information is available at:

<https://pubs.acs.org/10.1021/acs.est.4c03674>

### Notes

The authors declare no competing financial interest.

## ■ ACKNOWLEDGMENTS

This work was financially supported by the National Natural Science Foundation of China (Nos. 42073012, U2344228, and 41977288), Beijing Natural Science Foundation (No. 8212036), National Key Research & Development Program of China (Nos. 2023YFF0806004 and 2022YFC3701303), and the state Key Laboratory of Environmental Geochemistry (SKLEG2022214).

## ■ REFERENCES

(1) Rosman, K. J. R.; De Laeter, J. R. Low level determinations of environmental cadmium. *Nature* **1976**, *261*, 685–686.



- (2) Liu, X.; Hu, Q.; Yang, J.; Huang, S.; Wei, T.; Chen, W.; He, Y.; Wang, D.; Liu, Z. Selective cadmium regulation mediated by a cooperative binding mechanism in *CadR*. *Proc. Natl. Acad. Sci. U.S.A.* **2019**, *116* (41), 20398–20403.
- (3) Nordberg, G. F. Health hazards of environmental cadmium pollution. *Ambio* **1974**, *3*, 55–66.
- (4) Järup, L.; Åkesson, A. Current status of cadmium as an environmental health problem. *Toxicol. Appl. Pharmacol.* **2009**, *238*, 201–208.
- (5) Åkesson, A.; Barregard, L.; Bergdahl, I. A.; Nordberg, G. F.; Nordberg, M.; Skerfving, S. Non-renal effects and the risk assessment of environmental cadmium exposure. *Environ. Health Perspect.* **2014**, *122*, 431–438.
- (6) Salt, D. E.; Blaylock, M.; Kumar, N. P. B. A.; Dushenkov, V.; Ensley, B. D.; Chet, L.; Raskin, L. Phytoremediation: a novel strategy for the removal of toxic metals from the environment using plants. *Nat. Biotechnol.* **1995**, *13*, 468–474.
- (7) Yang, X. E.; Long, X. X.; Ye, H. B.; He, Z. L.; Calvert, D. V.; Stoffella, P. J. Cadmium tolerance and hyperaccumulation in a new Zn-hyperaccumulating plant species (*Sedum alfredii hance*). *Plant Soil.* **2004**, *259*, 181–189.
- (8) Guo, J. M.; Yang, J.; Yang, J. X.; Chen, T. B.; Guo, L. Subcellular cadmium distribution and antioxidant enzymatic activities in the leaves of four *Hylotelephium spectabile* populations exhibit differences in phytoextraction potential. *Int. J. Phytoremediat.* **2019**, *21*, 209–216.
- (9) Hou, D.; Wang, K.; Liu, T.; Wang, H.; Lin, Z.; Qian, J.; Lu, L.; Tian, S. Unique rhizosphere micro-characteristics facilitate phytoextraction of multiple metals in soil by the hyperaccumulating plant *Sedum alfredii*. *Environ. Sci. Technol.* **2017**, *51*, 5675–5684.
- (10) Peiffer, J. A.; Spor, A.; Koren, O.; Jin, Z.; Tringe, S. G.; Dangl, J. L.; Buckler, E. S.; Ley, R. E. Diversity and heritability of the maize rhizosphere microbiome under field conditions. *Proc. Natl. Acad. Sci. U. S. A.* **2013**, *110* (16), 6548–6553.
- (11) Xue, W. J.; Zhang, X.; Zhang, C. B.; Wang, C. R.; Huang, Y. C.; Liu, Z. Q. Mitigating the toxicity of reactive oxygen species induced by cadmium via restoring citrate valve and improving the stability of enzyme structure in rice. *Chemosphere.* **2023**, *327*, No. 138511.
- (12) Do Nascimento, C. W. A.; Amarasiriwardena, D.; Xing, B. S. Comparison of natural organic acids and synthetic chelates at enhancing phytoextraction of metals from a multi-metal contaminated soil. *Environ. Pollut.* **2006**, *140* (1), 114–123.
- (13) Lu, L. L.; Tian, S. K.; Yang, X. E.; Peng, H. Y.; Li, T. Q. Improved cadmium uptake and accumulation in the hyperaccumulator *Sedum alfredii*—the impacts of citric acid and tartaric acid. *J. Zhejiang Univ.-Sci. B* **2013**, *14*, 106–114.
- (14) Broadley, M. R.; White, P. J.; Hammond, J. P.; Zelko, I.; Lux, A. Zinc in plants. *New Phytol.* **2007**, *173* (4), 677–702.
- (15) Hall, J. L. Cellular mechanisms for heavy metal detoxification and tolerance. *J. Exp. Bot.* **2002**, *53*, 1–11.
- (16) Sun, G. L.; Reynolds, E. E.; Belcher, A. M. Designing yeast as plant-like hyperaccumulators for heavy metals. *Nat. Commun.* **2019**, *10*, 5080.
- (17) Clemens, S.; Palmgren, M. G.; Krämer, U. A long way ahead: understanding and engineering plant metal accumulation. *Trends Plant Sci.* **2002**, *7*, 309–315.
- (18) Hou, D. Y.; O'Connor, D.; Igalavithana, A. D.; Alessi, D. S.; Luo, J.; Tsang, D. C. W.; Sparks, D. L.; Yamauchi, Y.; Rinklebe, J.; Ok, Y. S. Metal contamination and bioremediation of agricultural soils for food safety and sustainability. *Nat. Rev. Earth Environ.* **2020**, *1*, 366–381.
- (19) Moore, K. L.; Chen, Y.; van de Meene, A. M. L.; Hughes, L.; Liu, W.; Geraki, T.; Mosselmans, F.; Mcgrath, S. P.; Grovenor, C.; Zhao, F. J. Combined NanoSIMS and synchrotron X-ray fluorescence reveal distinct cellular and subcellular distribution patterns of trace elements in rice tissues. *New Phytol.* **2014**, *201* (1), 104–115.
- (20) Lombi, E.; Scheckel, K. G.; Kempson, I. M. In situ analysis of metal(loid)s in plants: state of the art and artefacts. *Environ. Exp. Bot.* **2011**, *72* (1), 3–17.
- (21) Villafort Carvalho, M. T.; Pongrac, P.; Mumm, R.; van Arkel, J.; van Aelst, A.; Jeromel, L.; Vavpetič, P.; Pelicon, P.; Aarts, M. G. M. *Gomphrena clausenii*, a novel metalhypertolerant bioindicator species, sequesters cadmium, but not zinc, in vacuolar oxalate crystals. *New Phytol.* **2015**, *208* (3), 763–775.
- (22) Yang, W.; Lin, Y. T.; Zhang, J. C.; Hao, J. L.; Shen, W. J.; Hu, S. Precise micrometre-sized Pb-Pb and U-Pb dating with NanoSIMS. *J. Anal. At. Spectrom.* **2012**, *27* (3), 479–487.
- (23) Ouyang, X. X.; Ma, J.; Zhang, R.; Li, P.; Gao, M.; Sun, C. Q.; Weng, L. P.; Chen, Y. L.; Yan, S.; Li, Y. T. Uptake of atmospherically deposited cadmium by leaves of vegetables: Subcellular localization by NanoSIMS and potential risks. *J. Hazard. Mater.* **2022**, *431*, No. 128624.
- (24) Zhong, S.; Li, X.; Li, F.; Pan, D.; Liu, T.; Huang, Y.; Wang, Q.; Yin, H.; Huang, F. Cadmium isotope fractionation and gene expression evidence for tracking sources of Cd in grains during grain filling in a soil-rice system. *Sci. Total Environ.* **2023**, *873*, No. 162325.
- (25) Imseng, M.; Wiggenhauser, M.; Keller, A.; Müller, M.; Rehkämper, M.; Murphy, K.; Kreissig, K.; Frossard, E.; Wilcke, W.; Bigalke, M. Towards an understanding of the Cd isotope fractionation during transfer from the soil to the cereal grain. *Environ. Pollut.* **2019**, *244*, 834–844.
- (26) Wiggenhauser, M.; Bigalke, M.; Imseng, M.; Keller, A.; Rehkämper, M.; Wilcke, W.; Frossard, E. Using isotopes to trace freshly applied cadmium through mineral phosphorus fertilization in soil-fertilizer-plant systems. *Sci. Total Environ.* **2019**, *648*, 779–786.
- (27) Wiggenhauser, M.; Aucour, A.; Bureau, S.; Campillo, S.; Telouk, P.; Romani, M.; Ma, J. F.; Landrot, G.; Sarret, G. Cadmium transfer in contaminated soil-rice systems: Insights from solid-state speciation analysis and stable isotope fractionation. *Environ. Pollut.* **2021**, *269*, No. 115934.
- (28) Zhang, S. N.; Gu, Y.; Zhu, Z. L.; Hu, S. H.; Kopittke, P. M.; Zhao, F. J.; Wang, P. Stable isotope fractionation of cadmium in the soil-rice-human continuum. *Sci. Total Environ.* **2021**, *761*, No. 143262.
- (29) Zhong, S.; Li, X.; Li, F.; Liu, T.; Huang, F.; Yin, H.; Chen, G.; Cui, J. Water management alters cadmium isotope fractionation between shoots and nodes/leaves in a soil-rice system. *Environ. Sci. Technol.* **2021**, *55*, 12902–12913.
- (30) Zhong, S. X.; Fang, L. P.; Li, X. M.; Liu, T. X.; Wang, P.; Gao, R. C.; Chen, G. J.; Yin, H. M.; Yang, Y.; Huang, F.; Li, F. B. Roles of Chloride and sulfate ions in controlling cadmium transport in a soil-rice system as evidenced by the Cd isotope fingerprint. *Environ. Sci. Technol.* **2023**, *57* (46), 17920–17929.
- (31) Wiederhold, J. G. Metal stable isotope signatures as tracers in environmental geochemistry. *Environ. Sci. Technol.* **2015**, *49*, 2606–2624.
- (32) Gou, W. X.; Li, W.; Ji, J. F.; Li, W. Q. Zinc isotope fractionation during sorption onto Al oxides: atomic level understanding from EXAFS. *Environ. Sci. Technol.* **2018**, *52*, 9087–9096.
- (33) Yan, X. R.; Li, W.; Zhu, C. W.; Peacock, C. L.; Liu, Y. Z.; Li, H.; Zhang, J.; Hong, M.; Liu, F.; Yin, H. Zinc Stable Isotope Fractionation Mechanisms during Adsorption and Substitution in Iron (Hydr)oxides. *Environ. Sci. Technol.* **2023**, *57*, 6636–6646.
- (34) Li, S. Z.; Zhu, X. K.; Wu, L. H.; Luo, Y. M. Zinc, iron, and copper isotopic fractionation in *Elsholtzia splendens* Nakai: a study of elemental uptake and (re)translocation mechanisms. *J. Asian Earth Sci.* **2020**, *192*, 104227–104238.
- (35) Guelke, M.; Von Blanckenburg, F. Fractionation of stable iron isotopes in higher plants. *Environ. Sci. Technol.* **2007**, *41*, 1896–1901.
- (36) Pokharel, R.; Gerrits, R.; Schuessler, J. A.; Frings, P. J.; Sobotka, R.; Gorbushina, A. A.; von Blanckenburg, F. Magnesium stable isotope fractionation on a cellular level explored by cyanobacteria and black fungi with implications for higher plants. *Environ. Sci. Technol.* **2018**, *52*, 12216–12224.
- (37) Li, D. D.; Li, M. L.; Liu, W. R.; Qin, Z. Z.; Liu, S. A. Cadmium isotope ratios of standard solutions and geological reference materials

measured by MC-ICP-MS. *Geostand. Geoanal. Res.* **2018**, *42*, 593–605.

(38) Liu, M. S.; Zhang, Q.; Zhang, Y. N.; Zhang, Z. F.; Huang, F.; Yu, H. M. High-precision Cd isotope analyses of soil and rock reference materials by MC-ICP-MS with double spike correction. *Geostand. Geoanal. Res.* **2020**, *44*, 169–182.

(39) Song, W. R.; Gao, L. S.; Wei, C.; Wu, Y. Z.; Wen, H. J.; Huang, Z. L.; Zhang, J. W.; Chen, X. C.; Zhang, Y. X.; Zhu, C. W. Cd isotope constraints on metal sources of the Zhugongtang Zn–Pb deposit, NW Guizhou. *China. Ore Geology Reviews.* **2023**, *157*, No. 105426.

(40) Tan, D. C.; Zhu, J. M.; Wang, X. L.; Han, G. L.; Lu, Z.; Xu, W. P. High-sensitivity determination of Cd isotopes in low-Cd geological samples by double spike MC-ICP-MS. *J. Anal. At. Spectrom.* **2020**, *35*, 713–727.

(41) Zhu, C. W.; Wen, H. J.; Zhang, Y. X.; Huang, Z. L.; Cloquet, C.; Luais, B.; Yang, T. Cadmium isotopic constraints on metal sources in the Huize Zn–Pb deposit, SW China. *Geosci. Front.* **2021**, *12* (6), No. 101241.

(42) Wei, R. F.; Guo, Q. J.; Yu, G. R.; Kong, J.; Li, S. L.; Song, Z. L.; Hu, J.; Tian, L. Y.; Han, X. K.; Okoli, C. P. Stable isotope fractionation during uptake and translocation of cadmium by tolerant *Ricinus communis* and hyperaccumulator *Solanum nigrum* as influenced by EDTA. *Environ. Pollut.* **2018**, *236*, 634–644.

(43) Wei, R. F.; Guo, Q. J.; Tian, L. Y.; Kong, J.; Bai, Y.; Okoli, C. P.; Wang, L. Y. Characteristics of cadmium accumulation and isotope fractionation in higher plants. *Ecotox. Environ. Safte.* **2019**, *174*, 1–11.

(44) Pallavicini, N.; Engstrom, E.; Baxter, D. C.; Ohlander, B.; Ingri, J.; Rodushkin, I. Cadmium isotope ratio measurements in environmental matrices by MC-ICP-MS. *J. Anal. Atomic Spectrom.* **2014**, *29*, 1570–1584.

(45) Zhang, Y.; Wen, H.; Zhu, C.; Fan, H.; Cloquet, C. Cadmium isotopic evidence for the evolution of marine primary productivity and the biological extinction event during the Permian-Triassic crisis from the Meishan section, South China. *Chem. Geol.* **2018**, *481*, 110–118.

(46) Wombacher, F.; Rehkämper, M. Problems and suggestions concerning the notation of cadmium stable isotope compositions and the use of reference materials. *Geostand. Geoanal. Res.* **2004**, *28*, 173–178.

(47) Tartivel, R.; Tatin, R.; Delhaye, T.; Maupas, A.; Gendron, A.; Gautier, S.; Lavastre, O. Visualization and localization of bromotoluene distribution in *Hedera helix* using NanoSIMS. *Chemosphere.* **2012**, *89* (7), 805–809.

(48) Kilburn, M. R.; Clode, P. L. Elemental and isotopic imaging of biological samples using NanoSIMS. In: Kuo, J. (Ed.), *Electron Microscopy: Methods and Protocols*. Humana Press: Totowa, NJ. 2014, 733–755.

(49) Fu, X.; Dou, C.; Chen, Y.; Chen, X.; Shi, J.; Yu, M.; Xu, J. Subcellular distribution and chemical forms of cadmium in *Phytolacca americana* L. *J. Hazard. Mater.* **2011**, *186*, 103–107.

(50) Yang, J.; Guo, J.; Yang, J. Cadmium accumulation and subcellular distribution in populations of *Hylotelephium spectabile* (Bureau) H. Ohba. *Environ. Sci. Pollut. Res.* **2018**, *25*, 30917–30927.

(51) Smart, K. E.; Kilburn, M. R.; Salter, C. J.; Smith, J. A. C.; Grovenor, C. R. M. NanoSIMS and EPMA analysis of nickel localisation in leaves of the hyperaccumulator plant *Alyssum lesbiacum*. *Int. J. Mass Spectrom.* **2007**, *260*, 107–114.

(52) Tian, S. K.; Lu, L. L.; Labavitch, J.; Yang, X. E.; He, Z. L.; Hu, H. N.; Sarangi, R.; Newville, M.; Commisso, J.; Brown, P. Cellular Sequestration of Cadmium in the hyperaccumulator Plant Species *Sedum alfredii*. *Plant Physiol.* **2011**, *157* (4), 1914–1925.

(53) Van Belleghem, F.; Cuypers, A.; Semane, B.; Smeets, K.; Vangronsveld, J.; d'Haen, J.; Valcke, R. Subcellular localization of cadmium in roots and leaves of *Arabidopsis thaliana*. *New Phytol.* **2007**, *173*, 495–508.

(54) Pence, N. S.; Larsen, P. B.; Ebbs, S. D.; Letham, D. L. D.; Lasat, M. M.; Garvin, D. F.; Eide, D.; Kochian, L. V. The molecular physiology of heavy metal transport in the Zn/Cd hyperaccumulator *Thlaspi caerulescens*. *Proc. Natl. Acad. Sci. U. S. A.* **2000**, *97*, 4956–4960.

(55) Wójcik, M.; Vangronsveld, J.; D'Haen, J.; Tukiendorf, A. Cadmium tolerance in *Thlaspi caerulescens*: II. Localization of cadmium in *Thlaspi caerulescens*. *Environ. Exp. Bot.* **2005**, *53*, 163–171.

(56) Ramos, I.; Esteban, E.; Lucena, J. J.; Garate, A. Cadmium uptake and subcellular distribution in plants of *Lactuca sp.* Cd/Mn interaction. *Plant Sci.* **2002**, *162*, 761–767.

(57) Wu, F. B.; Dong, J.; Qian, Q. Q.; Zhang, G. P. Subcellular distribution and chemical form of Cd and Cd-Zn interaction in different barley genotypes. *Chemosphere.* **2005**, *60* (10), 1437–1446.

(58) Lu, L. L.; Tian, S. K.; Yang, X. E.; Li, T. Q.; He, Z. L. Cadmium uptake and xylem loading are active processes in the hyperaccumulator *Sedum alfredii*. *J. Plant Physiol.* **2009**, *166*, 579–587.

(59) Bolan, N.; Mahimairaja, S.; Kunhikrishnan, A.; Naidu, R. Sorption–bioavailability nexus of arsenic and cadmium in variable-charge soils. *J. Hazard. Mater.* **2013**, *261*, 725–732.

(60) Sauve, S.; Hendershot, W.; Allen, H. E. Solid-solution partitioning of metals in contaminated soils: Dependence on pH, total metal burden, and organic matter. *Environ. Sci. Technol.* **2000**, *34*, 1125–1131.

(61) Khaokaew, S.; Chaney, R. L.; Landrot, G.; Ginder-vogel, M.; Sparks, D. Speciation and release kinetics of cadmium in an alkaline paddy soil under various flooding periods and draining conditions. *Environ. Sci. Technol.* **2011**, *45* (10), 4249–4255.

(62) Imseng, M.; Wigganhauser, M.; Keller, A.; Müller, M.; Rehkämper, M.; Murphy, K.; Kreissig, K.; Frossard, E.; Wilcke, W.; Bigalke, M. Fate of Cd in Agricultural Soils: A Stable Isotope Approach to Anthropogenic Impact, Soil Formation, and Soil-Plant Cycling. *Environ. Sci. Technol.* **2018**, *52* (4), 1919–1928.

(63) Weiss, D. J.; Boye, K.; Caldelas, C.; Fendorf, S. Zinc isotope fractionation during early dissolution of biotite granite. *Soil Sci. Soc. Am. J.* **2014**, *78*, 171–179.

(64) Zhu, C. W.; Wen, H. J.; Zhang, Y. X.; Yin, R. S.; Cloquet, C. Cd isotope fractionation during sulfide mineral weathering in the Fule Zn-Pb-Cd deposit, Yunnan Province. *Southwest China. Sci. Total Environ.* **2018**, *616*, 64–72.

(65) Horner, T. J.; Lee, R. B. Y.; Henderson, G. M.; Rickaby, R. E. M. Nonspecific uptake and homeostasis drive the oceanic cadmium cycle. *Proc. Natl. Acad. Sci. U. S. A.* **2013**, *110* (7), 2500–2505.

(66) Yang, J.; Li, Y.; Liu, S.; Tian, H. Q.; Chen, C. Y.; Liu, J. M.; Shi, Y. L. Theoretical calculations of Cd isotope fractionation in hydrothermal fluids. *Chem. Geol.* **2015**, *391*, 74–82.

(67) Wei, R.; Guo, Q.; Wen, H.; Liu, C.; Yang, J.; Peters, M.; Hu, J.; Zhu, G.; Zhang, H.; Tian, L.; Han, X.; Ma, J.; Zhu, C.; Wan, Y. Fractionation of Stable Cadmium Isotopes in the Cadmium Tolerant *Ricinus communis* and hyperaccumulator *Solanum nigrum*. *Sci. Rep.* **2016**, *6*, 24309.

(68) Hinsinger, P. Bioavailability of trace elements as related to root-induced chemical changes in the rhizosphere. In *Trace Elements in the Rhizosphere*. CRC Press: Boca Raton, FL. 2001, 25–41.

(69) Bravin, M. N.; Garnier, C.; Lenoble, V.; Gérard, F.; Dudal, Y.; Hinsinger, P. Root-induced changes in pH and dissolved organic matter binding capacity affect copper dynamic speciation in the rhizosphere. *Geochim. Cosmochim. Acta* **2012**, *84*, 256–268.

(70) Wigganhauser, M.; Bigalke, M.; Imseng, M.; Müller, M.; Keller, A.; Murphy, K.; Kreissig, K.; Rehkämper, M.; Wilcke, W.; Frossard, E. Cadmium isotope fractionation in soil-wheat systems. *Environ. Sci. Technol.* **2016**, *50* (17), 9223–9231.

(71) Wasylenki, L. E.; Swihart, J. W.; Romaniello, S. J. Cadmium isotope fractionation during adsorption to Mn oxyhydroxide at low and high ionic strength. *Geochim. Cosmochim. Acta* **2014**, *140*, 212–226.

(72) Horner, T. J.; Rickaby, R. E. M.; Henderson, G. M. Isotopic fractionation of cadmium into calcite. *Earth Planet. Sci. Lett.* **2011**, *312*, 243–253.

(73) Zhou, J. W.; Moore, R. E. T.; Rehkämper, M.; Kreissig, K.; Coles, B.; Sun, Y. F.; Li, Z.; Luo, Y. M.; Christie, P.; Wu, L. H. Zinc supply affects cadmium uptake and translocation in the hyper-

accumulator *Sedum Plumbizincicola* as evidenced by isotope fractionation. *Environ. Sci. Technol.* **2023**, *57*, 5891–5902.

(74) Wiggerhauser, M.; Bigalke, M.; Imseng, M.; Keller, A.; Archer, C.; Wilcke, W.; Frossard, E. Zinc isotope fractionation during grain filling of wheat and a comparison of zinc and cadmium isotope ratios in identical soil-plant systems. *New Phytol.* **2018**, *219* (1), 195–205.

(75) Mendoza-Cozatl, D. G.; Jobe, T. O.; Hauser, F.; Schroeder, J. I. Long-distance transport, vacuolar sequestration, tolerance, and transcriptional responses induced by cadmium and arsenic. *Curr. Opin. Plant Biol.* **2011**, *14*, 554–562.

(76) Peng, J. S.; Wang, Y. J.; Ding, G.; Ma, H. L.; Zhang, Y. J.; Gong, J. M. A pivotal role of cell wall in cadmium accumulation in the Crassulaceae hyperaccumulator *Sedum plumbizincicola*. *Mol. Plant.* **2017**, *10* (5), 771–774.

(77) Cheng, M. M.; Wang, P.; Kopittke, P. M.; Wang, A. A.; Sale, P. W. G.; Tang, C. X. Cadmium accumulation is enhanced by ammonium compared to nitrate in two hyperaccumulators, without affecting speciation. *J. Exp. Bot.* **2016**, *67* (17), 5041–5050.

(78) Malekzadeh, R.; Shahpiri, A. Independent metal-thiolate cluster formation in c-terminal cys-rich region of a rice type 1 metallothionein isoform. *Int. J. Biol. Macromol.* **2017**, *96*, 436–441.

(79) Samuel, M. S.; Datta, S.; Khandge, R. S.; Selvarajan, E. A state of the art review on characterization of heavy metal binding metallothioneins proteins and their wide spread applications. *Sci. Total Environ.* **2021**, *775*, No. 145829.

(80) Zhong, S. X.; Li, X. M.; Li, F. B.; Huang, Y. M.; Liu, T. X.; Yin, H. M.; Qiao, J. T.; Chen, G. J.; Huang, F. Cadmium uptake and transport processes in rice revealed by stable isotope fractionation and Cd-related gene expression. *Sci. Total Environ.* **2022**, *806*, No. 150633.